COUPLING OF MULTIPHASE FLOW MODELS

Annalisa Ambroso[1],
CEA-Saclay, F-91191 Gif-sur-Yvette, France,
Phone: +33 (0) 1 6908 1686, Fax: +33 (0) 1 6908 8568, annalisa.ambroso@cea.fr

Christophe Chalons, Frédéric Coquel, Edwige Godlewski, Frédéric Lagoutière, Pierre-Arnaud Raviart, Nicolas Seguin, Laboratoire Jacques-Louis Lions UMR 7598 Boîte courrier 187, 75252 Paris Cedex 05 France, chalons@math.jussieu.fr, coquel@ann.jussieu.fr, godlewski@ann.jussieu.fr, lagoutie@ann.jussieu.fr, raviart@ann.jussieu.fr, seguin@ann.jussieu.fr,

Jean-Marc Hérard, EDF DRD 6, quai Watier, F-78400 Chatou, France, jean-marc.herard@edf.fr

ABSTRACT

When modelling and simulating complex systems, one often needs to use specific models for each component to take into account their behavior. This is the case, for instance, for the modelling of the coolant flow in a Pressurized Water Reactor. In the frame of the NEPTUNE project, it is clear that to obtain a complete and coherent description of the system as a whole, one needs to couple these different models. We thus consider two separate domains sharing an interface. In each one, a different model is used to describe the flow. We want to single out the information to be transmitted through the interface in a way to obtain a coherent description of the unsteady flow. As an example, we consider a one-dimensional flow described everywhere by the same set of equations. An interface separates a region where the fluid is described by a given EOS and another region with a different EOS. This is a very common case in practice, since the tabulated thermodynamic functions used by different codes present some discrepancies. We compare different coupling schemes, originated from two distinct and relevant modelling choices and we show that they can lead to different solutions.

KEYWORDS

Model Coupling, Gas Dynamics, Two-Phase Flow, Finite Volumes

INTRODUCTION

Coupling different thermal-hydraulic models has become a key issue in the development of a new generation of two-phase flow codes for nuclear reactors as in NEPTUNE, see (Guelfi, 2005).
In these codes, multiple modelling scales are applied to describe the flow. For instance, different models can be used to describe each reactor component to take into account their specific behavior or small scale models can be used, locally, to obtain a better geometric description of the flow.
When these models are put side to side to describe the whole circuit, we face the problem of coupling. In particular we need to identify which is the information to be transmitted at each coupling interface to have a coherent description of the system.

In the framework of NEPTUNE project, some tests of interface coupling have been implemented (Boudier & Laviéville, 2004) and the results obtained give rise to some interesting questions and show that a deep analysis of the problem is necessary.
Even in some very simple cases, the coupling can be source of errors. Actually, when computing a solution of a coupled problem, we are intervening on three stages. The first is on the level of the physical modelling, when we define which is the information to be transmitted at the interface. The second is

[1]Corresponding author

linked with the analysis of the chosen coupled model, which can admit multiple solutions. Finally, problems can arise in the numerical approximation of the model.

In Section 1 we list some aspects of the coupling problem. As it will become apparent, different difficulties must be faced to couple two generic models as the ones encountered in the simulation of the coolant flow in a nuclear reactor. In order to better understand their role in the generic coupling problem, we choose to focus on each one of them separately, in a first time.

On the mathematical point of view, two main approaches can be singled out to model the coupling problem. On the one hand, a global model can be used to describe the flow at the interface of coupling, while the distinct models on each side of it must be seen as deriving from this global model. On the other hand, the coupling problem can be interpreted as the juxtaposition of two initial boundary problems (one on each side of the interface). The coupling being insured by the choice of "compatible" boundary conditions to be imposed at the interface. These approaches are described in Section 2.

In Section 3, we discuss one particular coupling problem. We consider a one-dimensional flow described everywhere by the same set of equations. An interface at $x = 0$ separates a region where the fluid is described by a given EOS and another region where the EOS is slightly modified. This is a very common case in practice, since the tabulated thermodynamic functions used by different codes present some discrepancies. We describe and compare the different coupling techniques we propose in this example. Numerical results are presented in Section 4.

1 EXAMPLES OF INTERFACE COUPLING OF MODELS

Building a code to have predictive computations of the flow in the primary coolant circuit of a pressurized power reactor requires using different codes involving different systems of PDE on each side of a "fictitious" interface. The model chosen to describe the flow in pipes may for instance be a six-equation two-fluid model, whereas the one considered in the core may be a three-equation model (to account for total mass, total energy and total momentum of the water-vapor mixture). The problem clearly is the following: what kind of information should be transferred through the interface, in such a way that incoming/outcoming information traveling through both codes should not be polluted by the neighboring code? This leads directly to the mathematical question of existence and uniqueness of physically relevant solutions of the whole problem including this new "interface" information. Moreover, efficient, stable and accurate ways to account for this "interface" information need to be defined. We itemize below some examples of the different models we need to couple.

1.1 Open medium / porous medium

A first problem which has been identified concerns the transmission of information through a porous interface. The flow on the left side of a steady interface is governed by standard Euler equations in a free medium, whereas it enters a porous medium on the right. Thus the only heterogeneity pertains to the porosity. In (Hérard, 2004), the whole is modeled according to ideas similar to those developed by Greenberg and Leroux (Greenberg & LeRoux, 1996). This approach suggests a connection through the interface when Genuinely Non Linear fields do not overlap the steady interface. Some possible numerical ways to account for this have been defined and compared with approaches where the interface is thickened. When some GNL field overlaps the interface, the agreement of the numerical approximation with the entropy inequality has been checked for each scheme.

1.2 Flows through pipes and reactors

A second straightforward problem immediately arises when connecting the CATHARE code and the THYC code (or alternatively the FLICA code) for instance. In that case, one has to cope with a one-dimensional model (on the left side of a fictitious interface) which suddenly becomes three-dimensional. One may a priori think that no problem will occur when the flow comes from the left to the right (in the

common sense, i.e. $U > 0$), and that on the contrary some pollution of the numerical signal cannot be avoided when ($U < 0$). The work (Hérard & Hurisse, 2004a) partially investigates this topic, and shows that previous ideas give fair results from an engineering point of view.

1.3 The influence of thermodynamical EOS

A commonly disregarded point is the sensibility of computational results to the choice of EOS in codes. During the last thirty years, various thermodynamical approaches have been proposed and implemented in internal softwares in different companies. The direct consequence is that the interfacial coupling of different codes involving these different softwares may result in unexpected disturbances around the interface, which in addition may propagate through (and reflect on) the fictitious boundary. It thus urges to examine the coupling of similar equations with arbitrary jumps of coefficients, retaining rather simple equations of state. This problem is treated in detail in Section 3.

1.4 Relaxed / unrelaxed models

As it has been underlined above, we also need to investigate the coupling of totally distinct models in a one dimensional open medium frame. The main goal of such concern is of course the clear definition of the information to be exchanged between a six-equation two-fluid model and a four-equation homogeneous model. For that purpose, we must first examine: (i) the coupling of a relaxed and unrelaxed model (typically HEM and HRM) ; (ii) the coupling of first order homogeneous models (typically a two-fluid model and a homogeneous three-equation model, assuming that no mass transfer occurs during the computation). We also have to check what is the best numerical strategy in order to account for relaxation terms (mass transfer, drag effects, energy transfer) in an unsteady (or steady) computation, which is clearly linked to point (i). The results of (Hérard & Hurisse, 2004b) suggest that different numerical approaches should be retained depending whether one focuses on steady or unsteady coupling. Point (i) is currently under investigation (Ambroso *et al.* , 2005), (Hurisse, n.d.).

2 MATHEMATICAL MODEL OF THE COUPLED PROBLEM

We describe in this section the general framework of the coupling problem and the two main approaches to treat it. We consider a domain $\Omega \in \mathbb{R}^n$ divided in two sub-domains Ω_1 and Ω_2 by an interface.
A flow in Ω is described by means of two different models on Ω_1 and Ω_2. We call W_α ($\alpha = 1, 2$) the vector of the unknowns describing the fluid on Ω_α.
The most general case consists in taking $W_1 \in \mathbb{R}^q$ and $W_2 \in \mathbb{R}^p$ with $q \neq p$, *i.e.* the number of equations in the models is not the same.
The problem reads, in this case

$$\begin{array}{l|l}
\mathbf{W}_1 \in \mathbb{R}^q \,, & \mathbf{W}_2 \in \mathbb{R}^p \,, \\
\partial_t \mathbf{W}_1 + \sum_{i=1}^{n} \partial_{x_i} \mathbf{F}_{i,1}(\mathbf{W}_1) + & \partial_t \mathbf{W}_2 + \sum_{i=1}^{n} \partial_{x_i} \mathbf{F}_{i,2}(\mathbf{W}_2) + \\
+ \sum_{i=1}^{n} \mathbf{G}_{i,1} \partial_{x_i} \mathbf{W}_1 = \mathbf{S}_1(\mathbf{W}_1) \,, & + \sum_{i=1}^{n} \mathbf{G}_{i,2} \partial_{x_i} \mathbf{W}_2 = \mathbf{S}_2(\mathbf{W}_2) \,, \\
\text{on} \quad \mathbb{R}_+ \times \Omega_1 \,, & \text{on} \quad \mathbb{R}_+ \times \Omega_2 \,,
\end{array} \tag{1}$$

where $\mathbf{F}_{i,\alpha}$, $\sum_{i=1}^{n} \mathbf{G}_{i,\alpha} \partial_{x_i} \mathbf{W}_\alpha$ and S_α are respectively the conservative flux, the non-conservative term and the source term on Ω_α.

The main problem is to single out the information to be transmitted through the interface, for every time t in the form of a mathematical condition, in order to obtain a coherent description of the flow

without modifying the two models and without having to solve one (or both) of the models on the whole domain Ω.

Many techniques can be proposed, we cast them in two main strategies. The first one, called *flux coupling* in the following, consists in identifying a global model for the flow. This global model dictates the transmission law at the interface, while the models used on each side of it must be recovered by a limiting procedure.

The other way to couple two models communicating through an interface, is to consider them as two separate initial boundary value problems and to give *reasonable* conditions on the interface for each one of them to reestablish the connection for the global problem.
With this point of view, the coupling can be insured by choosing to impose a continuity condition of the state-variables of the fluid at the crossing of the interface. For this reason, we call this method *intermediate state coupling*.
A theoretical analysis of this coupling technique can be found in (Godlewski & Raviart, 2004) and (Godlewski *et al.* , 2005).

In general, the choice of the strategy to follow must depend on the particular coupling problem it applies to.

We propose to characterize each technique by its consequences on the properties of the solutions of the coupled model. In particular, we will focus in the following on the conservation of physical quantities (and of energy in particular) and on the capacity of reproducing steady state solutions.

With this aim, we will analyze a particular problem and describe three numerical algorithms to solve it. Two of them are to be considered as flux coupling techniques, while the third is a state coupling one.

3 COUPLING OF TWO SYSTEMS OF GAS DYNAMICS WITH DIFFERENT EQUATIONS OF STATE

We consider the one dimensional motion of a fluid described by the following Euler system:

$$\begin{cases} \partial_t \rho + \partial_x(\rho u) = 0, \\ \partial_t(\rho u) + \partial_x(\rho u^2 + p) = 0, \\ \partial_t(\rho E) + \partial_x(\rho E + p)u = 0. \end{cases} \tag{2}$$

The first equation expresses the conservation of the mass of the fluid. The second and the third govern, respectively, the conservation of momentum ρu and total energy ρE. The pressure p is linked to the vector of the unknowns $\mathbf{u} = (\rho, \rho u, \rho E)$ of the system by a generic analytical equation of state

$$p = p(\rho, \varepsilon), \quad \rho\varepsilon = \rho E - \frac{1}{2}\rho u^2. \tag{3}$$

The domain $\Omega = \mathbb{R}$ is divided in two subdomains $\mathbb{R}^{-,*}$ and $\mathbb{R}^{+,*}$ separated by the interface $x = 0$.
The model for the flow on each side of the interface is the same, but we consider the case in which a small discrepancy in the description of the thermodynamic properties of the fluid is present. This is translated by taking two slightly different equations of state on the left and on the right of $x = 0$. Therefore, we note $p_1 = p_1(\rho, \varepsilon)$ the thermodynamic law which applies on the left domain and $p_2 = p_2(\rho, \varepsilon)$ the thermodynamic law on the right domain.

The coupling problem reads

$$\begin{array}{c|c} \Omega_1 = \mathbb{R}^{-,*} & \Omega_2 = \mathbb{R}^{+,*} \\ \left\{ \begin{array}{l} \partial_t \rho + \partial_x(\rho u) = 0, \\ \partial_t(\rho u) + \partial_x(\rho u^2 + p_1) = 0, \\ \partial_t(\rho E) + \partial_x(\rho E + p_1)u = 0. \end{array} \right. & \left\{ \begin{array}{l} \partial_t \rho + \partial_x(\rho u) = 0, \\ \partial_t(\rho u) + \partial_x(\rho u^2 + p_2) = 0, \\ \partial_t(\rho E) + \partial_x(\rho E + p_2)u = 0. \end{array} \right. \\ p_1 = p_1(\rho, \varepsilon), & p_2 = p_2(\rho, \varepsilon), \end{array} \tag{4}$$

With clear notation, we write it also in condensed form:

$$\partial_t \mathbf{u} + \partial_x \mathbf{f_1}(\mathbf{u}) = 0, \quad \text{on } \Omega_1 \quad | \quad \partial_t \mathbf{u} + \partial_x \mathbf{f_2}(\mathbf{u}) = 0, \quad \text{on } \Omega_2$$

Let Δt and Δx be the time and space steps. The grid points $(x_j)_{j\in\mathbb{Z}}$ are defined by $x_j = j\Delta x$. For all $j \in \mathbb{Z}$ and all $n \in \mathbb{N}$, we set

$$x_{j+1/2} = x_j + \frac{\Delta x}{2}, \quad t^n = n\Delta t,$$

and we consider the following computational grid $\mathbb{R}_x \times \mathbb{R}_t^+$:

$$\mathbb{R}_x \times \mathbb{R}_t^+ = \bigcup_{j\in\mathbb{Z}} \bigcup_{n\geq 0} C_{j+1/2}^n, \quad C_{j+1/2}^n = [x_j, x_{j+1}[\times[t^n, t^{n+1}[.$$

The numerical solutions $\mathbf{u}_{\Delta t,\Delta x}(x,t)$ of the problem corresponding to the initial condition $\mathbf{u}_0$ are given by piecewise constant functions on each $C_{j+1/2}^n$:

$$\mathbf{u}_{\Delta t,\Delta x}(x,t) = \mathbf{u}_{j+1/2}^n \text{ for } (x,t) \in C_{j+1/2}^n.$$

At $t = 0$, we set

$$\mathbf{u}_{j+1/2}^0 = \frac{1}{\Delta x} \int_{x_j}^{x_{j+1}} \mathbf{u}_0(x)dx, \quad j \in \mathbb{Z}.$$

Therefore, the grid points x_j correspond to the interface of the grid cells. The centers of the cells are identified by the subscripts $(j + 1/2)$. We remark that the coupling interface is in x_0 and the point x_i belongs to the left domain (respectively to the right domain) if $i < 0$ (respectively $i > 0$).

3.1 Incompatibility between uniform pressure profiles and energy conservation

Before we propose some numerical schemes for the computation of the solutions of the coupling problem (4), we want to make an important remark on the continuous level.
Problem (4) is the model of the flow of a fluid which presents a discrepancy in its thermodynamic description when it passes through an interface. This unphysical situation has some consequences on the properties of the solutions of Problem (4). In particular, we show that, if we want uniform pressure profiles to be steady state solutions for (4), we need to accept a non-conservative model for the interface.

We consider a uniform profile as initial condition for the coupling problem (4), *i.e.*, for all $x \in \mathbb{R}$:

$$\left\{ \begin{array}{rcl} \rho(x) & = & \rho^0, \\ u(x) & = & u^0, \\ p(x) & = & p^0, \end{array} \right. \tag{5}$$

where $u^0 \neq 0$. This profile is a steady solution of the two problems on each side of the interface taken separately. We expect it to be a steady state for the flow in the global model and therefore a solution for Problem (4) for all time t.

We analyze the behavior of the total energy ρE for this stationary solution. First we remark that, since the equations of state $p_1(\rho,\varepsilon)$ and $p_2(\rho,\varepsilon)$ are different on each side of the interface, the corresponding internal energies ε_1 and ε_2 are different.
We write the energy balance on the volume $V=[-1/2,1/2]\times[0,T]$ with $T>0$:

$$EnergyBalance = A(T) - A(0) + B(1/2) - B(-1/2)\ , \tag{6}$$

with

$$A(t) = \int_{-1/2}^{1/2} \rho E(x,t)dx \quad \text{and} \quad B(x) = \int_0^T (\rho E u + pu)(x,t)dt.$$

This balance should be identically zero if total energy were conserved.
When we evaluate this balance in the case of the solution (5), we obtain

$$EnergyBalance = \rho^0 u^0 (\varepsilon_2 - \varepsilon_1)T \neq 0. \tag{7}$$

Therefore the total energy ρE is not conserved, while ρ and ρu are trivially conserved. Moreover, from Equation (7) it is clear that the conservation error is a direct consequence of the change of equation of state and it vanishes only if the two EOS are the same or if the flow does not cross the interface (*i.e.* if $u^0=0$).
This back of the envelope computation shows that, when the equation of state has jumps, it is impossible to capture uniform pressure and velocity profiles if we impose the strict conservation of energy.
The same conclusion holds for material fronts, i.e. for discontinuous density profiles propagating at uniform velocity and uniform pressure. We will see the consequences of this remark in the following sections when we compute the solutions of Problem (4) following different strategies.

3.2 Flux coupling

We study now a flux coupling strategy. As global model for the coupling problem (4) we propose the following relaxation system

$$\begin{cases} \partial_t \rho + \partial_x(\rho u) = 0, \\ \partial_t(\rho u) + \partial_x(\rho u^2 + p) = 0, \\ \partial_t(\rho E) + \partial_x(\rho E + p)u = 0, \\ \partial_t(\rho Y) + \partial_x(\rho Y u) = \lambda\rho(Y_0 - Y), \end{cases} \tag{8}$$

where Y is a 'color' variable, the pressure p is given by the relation

$$p = (1-Y)p_1 + Yp_2$$

and

$$Y_0 = \begin{cases} 0 & \text{if} \quad x<0, \\ 1 & \text{if} \quad x>0. \end{cases}$$

We remark that, in the limit $\lambda\to\infty$, usually called 'equilibrium', this system formally converges toward (4).
With clear notations, we rewrite the system (8) in the following short form

$$\partial_t \mathbf{v} + \partial_x \mathbf{F}(\mathbf{v}) = \lambda\mathcal{R}(\mathbf{v}). \tag{9}$$

Remark: We want to notice that different choices for the global model could have been made, for instance, we could have considered the following system

$$\begin{cases} \partial_t \rho + \partial_x(\rho u) = 0, \\ \partial_t(\rho u) + \partial_x(\rho u^2 + p) = 0, \\ \partial_t(\rho E) + \partial_x(\rho E + p)u = 0, \\ \partial_t Y = 0, \end{cases}$$

with the same definition of p as above. Even if this choice looks simpler, on the mathematical and numerical point of view, this system is much more complicated than the one we considered since it hides a possible resonance phenomenon. This approach has nonetheless been considered in the context of the coupling of porous and open media in (Hérard, 2004).

3.2.1 Description of the algorithm

We describe briefly the algorithm associated with the Relaxation model (8). We define a piecewise constant function $\mathbf{v}_{\Delta t,\Delta x}$ by

$$\mathbf{v}_{\Delta t,\Delta x}(x,t) = \mathbf{v}^n_{j+1/2} = \begin{pmatrix} \mathbf{u}^n_{j+1/2} \\ (\rho Y)^n_{j+1/2} \end{pmatrix} \text{ for } (x,t) \in C^n_{j+1/2}.$$

This function is supposed to be at equilibrium, *i.e.*

$$(\rho Y)^n_{j+1/2} = \begin{cases} 0 & \text{if } \ j<0, \\ \rho^n_{j+1/2} & \text{if } \ j \geq 0. \end{cases}$$

Starting from a known approximated solution $\mathbf{u}_{\Delta t,\Delta x}(x,t^n)$ at a time $t^n \geq 0$, we propose to compute the solution at time t^{n+1} in two steps.

First step: evolution ($t^n \to t^{n+1-}$)
For this step, we take $\lambda = 0$ and we let the solution evolve following the system

$$\partial_t \mathbf{v} + \partial_x \mathbf{F}(\mathbf{v}) = 0.$$

To solve numerically this system, the classical Riemann solvers can be used (Roe, relaxation method, ...). For the numerical tests we present in the next section, we used a Lagrange+Projection method (see (Godlewski & Raviart, 1996)) that we applied in two different ways. They will be detailed in the following two sections.
For a $(2k+1)$-points conservative scheme, we have

$$\mathbf{v}^{n+1-}_{j+1/2} = \mathbf{v}^n_{j+1/2} - \frac{\Delta t}{\Delta x}(\mathbf{G}(\mathbf{v}^n_{j-k+3/2},...,\mathbf{v}^n_{j+k+1/2}) - \mathbf{G}(\mathbf{v}^n_{j-k+1/2},...,\mathbf{v}^n_{j+k-1/2})), \tag{10}$$

where the numerical flux function g depends on the chosen method.
Clearly, $\mathbf{u}^{n+1-}_{j+1/2}$ is defined by the relation

$$\mathbf{v}^{n+1-}_{j+1/2} = \begin{pmatrix} \mathbf{u}^{n+1-}_{j+1/2} \\ (\rho Y)^{n+1-}_{j+1/2} \end{pmatrix}.$$

Second step : relaxation ($t^{n+1-} \to t^{n+1}$)
This second step consists in a projection of the function $\mathbf{v}_{\Delta t,\Delta x}(x,t^{n+1-})$, obtained from the previous step, on the equilibrium position $\lambda = +\infty$. More precisely, we set, for all $j \in \mathbb{Z}$:

$$\begin{gathered} \mathbf{v}^{n+1}_{j+1/2} = \begin{pmatrix} \mathbf{u}^{n+1}_{j+1/2} \\ (\rho Y)^{n+1}_{j+1/2} \end{pmatrix} \quad \text{with} \quad \mathbf{u}^{n+1}_{j+1/2} = \mathbf{u}^{n+1-}_{j+1/2} \\ \text{and} \quad (\rho Y)^{n+1}_{j+1/2} = \begin{cases} 0 & \text{if } \ j<0, \\ \rho^{n+1}_{j+1/2} & \text{if } \ j \geq 0. \end{cases} \end{gathered} \tag{11}$$

This is equivalent to solving the following ODE system with $\lambda = +\infty$:

$$\begin{cases} \partial_t \rho = 0, \\ \partial_t(\rho u) = 0, \\ \partial_t(\rho E) = 0 \\ \partial_t(\rho Y) = \lambda \rho (Y_0 - Y). \end{cases} \tag{12}$$

Therefore, the global algorithm can be interpreted as a splitting technique applied to (8): first we solve its convective part, and in a second time its source term in the $\lambda \to \infty$ regime.

Remark: It is clear that the approximated solution $\mathbf{u}_{\Delta t,\Delta x}$ evolves in a conservative way when the scheme used to perform the first step is conservative.

3.2.2 Totally conservative Lagrange+Projection scheme

We focus now on the first step of the algorithm of flux coupling described above. First, we describe a totally conservative Lagrange+Projection strategy for the resolution of the following system:

$$\begin{cases} \partial_t \rho + \partial_x(\rho u) = 0, \\ \partial_t(\rho u) + \partial_x(\rho u^2 + p) = 0, \\ \partial_t(\rho E) + \partial_x(\rho E + p)u = 0, \\ \partial_t(\rho Y) + \partial_x(\rho Y u) = 0, \end{cases} \tag{13}$$

with $p = (1-Y)p_1 + Yp_2$.
We consider a piecewise constant numerical approximation $\mathbf{v}^n$ of the exact solution $\mathbf{v}$ at time t^n of System (13):

$$\mathbf{v}(x,t^n) \approx \mathbf{v}^n(x) = \mathbf{v}^n_{j+1/2} \text{ for } x \in [x_j, x_{j+1}[.$$

The approximated solution at time t^{n+1} is computed in two steps.

Lagrange step
We write system (13) in Lagrangian coordinates. We denote by ξ the Lagrangian coordinates associated with the velocity field u and $\tau = 1/\rho$ the specific volume. System (13) reads

$$\begin{cases} \rho_0 \partial_t \tau - \partial_\xi u = 0, \\ \rho_0 \partial_t u + \partial_\xi p = 0, \\ \rho_0 \partial_t E + \partial_\xi pu = 0, \\ \partial_t Y = 0, \end{cases} \tag{14}$$

where $\rho_0 = \rho(\xi, 0)$. We solve (14) by an acoustic scheme:

$$\begin{cases} \tau^{n+1-}_{j+1/2} = \tau^n_{j+1/2} + \dfrac{\Delta t}{\rho^n_{j+1/2}\Delta x}(u^n_{j+1} - u^n_j), \\ u^{n+1-}_{j+1/2} = u^n_{j+1/2} - \dfrac{\Delta t}{\rho^n_{j+1/2}\Delta x}(p^n_{j+1} - p^n_j), \\ E^{n+1-}_{j+1/2} = E^n_{j+1/2} - \dfrac{\Delta t}{\rho^n_{j+1/2}\Delta x}((pu)^n_{j+1} - (pu)^n_j), \\ Y^{n+1-}_{j+1/2} = Y^n_{j+1/2}, \end{cases}$$

with

$$\begin{cases} u^n_j = \dfrac{1}{2}(u^n_{j-1/2} + u^n_{j+1/2}) + \dfrac{1}{2(\rho c)^n_j}(p^n_{j-1/2} - p^n_{j+1/2}), \\ p^n_j = \dfrac{1}{2}(p^n_{j-1/2} + p^n_{j+1/2}) + \dfrac{(\rho c)^n_j}{2}(u^n_{j-1/2} - u^n_{j+1/2}), \end{cases}$$

where $(\rho c)^n_j$ is a local approximation of the Lagrangian sound speed:

$$(\rho c)^n_j = \max((\rho c)^n_{j-1/2}, (\rho c)^n_{j+1/2}).$$

The pressures $p^n_{j+1/2}$ are computed by means of the relation:

$$p^n_{j+1/2} = (1 - Y^n_{j+1/2})p_1(\rho^n_{j+1/2}, \varepsilon^n_{j+1/2}) + Y^n_{j+1/2}p_2(\rho^n_{j+1/2}, \varepsilon^n_{j+1/2}),$$

where

$$\varepsilon^n_{j+1/2} = \rho^n_{j+1/2}E^n_{j+1/2} - \frac{1}{2}\rho^n_{j+1/2}(u^n_{j+1/2})^2$$

The grid points x_j move at the fluid velocity, which is approximated by u^n_j. The quantities $\rho^{n+1-}_{j+1/2} = 1/\tau^{n+1-}_{j+1/2}$, $(\rho u)^{n+1-}_{j+1/2} = \rho^{n+1-}_{j+1/2} \times u^{n+1-}_{j+1/2}$, $(\rho E)^{n+1-}_{j+1/2} = \rho^{n+1-}_{j+1/2} \times E^{n+1-}_{j+1/2}$ and $(\rho Y)^{n+1-}_{j+1/2} = \rho^{n+1-}_{j+1/2} \times Y^{n+1-}_{j+1/2}$ are approximations of the exact solution on a 'Lagrange-grid' x^*_j defined by $x^*_j = x_j + u^n_j \Delta t$.

Projection step

The functions obtained in the previous step are constant on the Lagrangian cells. We project them on the Eulerian grid x_j. We set

$$\varphi_{j+1/2}^{n+1} = \frac{1}{\Delta x}\int_{x_j}^{x_{j+1}} \varphi^{n+1-}(x)dx \quad \text{with} \quad \varphi = \rho, \rho u, \rho E, \rho Y,$$

which gives

$$\varphi_{j+1/2}^{n+1} = \frac{1}{\Delta x}\{\Delta x_{j+1/2}^{*}\varphi_{j+1/2}^{n+1-} - \Delta t(u_{j+1}^{n}\varphi_{j+1+\alpha_{j+1,n}}^{n+1-} - u_j^n\varphi_{j+\alpha_{j,n}}^{n+1-})\}$$

with

$$\Delta x_{j+1/2}^{*} = x_{j+1}^{*} - x_j^{*}, \quad \text{and} \quad \alpha_{j,n} = \begin{cases} -1/2 & \text{if} \quad u_j^n > 0, \\ 1/2 & \text{if} \quad u_j^n < 0. \end{cases}$$

Finally, we get for $\mathbf{v}_{j+1/2}^n$:

$$\begin{cases} \rho_{j+1/2}^{n+1} = \rho_{j+1/2}^{n} - \dfrac{\Delta t}{\Delta x}(u_{j+1}^{n}\rho_{j+1+\alpha_{j+1,n}}^{n+1-} - u_j^n\rho_{j+\alpha_{j,n}}^{n+1-}), \\ (\rho u)_{j+1/2}^{n+1} = (\rho u)_{j+1/2}^{n} - \dfrac{\Delta t}{\Delta x}(u_{j+1}^{n}(\rho u)_{j+1+\alpha_{j+1,n}}^{n+1-} + p_{j+1}^{n} - u_j^n(\rho u)_{j+\alpha_{j,n}}^{n+1-} - p_j^n), \\ (\rho E)_{j+1/2}^{n+1} = (\rho E)_{j+1/2}^{n} - \dfrac{\Delta t}{\Delta x}(u_{j+1}^{n}(\rho E)_{j+1+\alpha_{j+1,n}}^{n+1-} + (pu)_{j+1}^{n} - u_j^n(\rho E)_{j+\alpha_{j,n}}^{n+1-} - (pu)_j^n), \\ (\rho Y)_{j+1/2}^{n+1} = (\rho Y)_{j+1/2}^{n} - \dfrac{\Delta t}{\Delta x}(u_{j+1}^{n}(\rho Y)_{j+1+\alpha_{j+1,n}}^{n+1-} - u_j^n(\rho Y)_{j+\alpha_{j,n}}^{n+1-}), \end{cases} \tag{15}$$

We remark that this scheme is completely conservative (*i.e.* conservative for all the variables). The associated numerical flux will be noted $\mathbf{g}^{LPc}$. In the following we will use the condensed form for (15):

$$\mathbf{v}_{j+1/2}^{n+1} = \mathbf{v}_{j+1/2}^{n} - \tfrac{\Delta t}{\Delta x}(\mathbf{g}^{LPc}(\mathbf{v}_{j-1/2}^{n}, \mathbf{v}_{j+1/2}^{n}, \mathbf{v}_{j+3/2}^{n}, \mathbf{v}_{j+5/2}^{n}) - \mathbf{g}^{LPc}(\mathbf{v}_{j-3/2}^{n}, \mathbf{v}_{j-1/2}^{n}, \mathbf{v}_{j+1/2}^{n}, \mathbf{v}_{j+3/2}^{n})). \tag{16}$$

The general flux coupling algorithm which is obtained is also conservative, but we will see in Section 4 that it presents some problems for the simulation of steady states, as it has to be expected from our discussion in Section 3.1.

3.2.3 Lagrange+Projection scheme with mean pressure projection

A detailed analysis of the algorithm proposed in the preceding section shows that the problems it presents for the computation of steady states can be charged on the projection step for the variable ρE. We propose here to modify this step in a way to obtain a pseudo-conservative scheme which can capture uniform profiles in p.

The Lagrangian step is unmodified. We focus only on the projection step.

For the variables ρ, ρu and ρY, no modification is required:

$$\varphi_{j+1/2}^{n+1} = \frac{1}{\Delta x}\int_{x_j}^{x_{j+1}} \varphi^{n+1-}(x)dx \quad \text{with} \quad \varphi = \rho, \rho u, \rho Y.$$

We propose to modify the computation of ρE on the cells that touch the coupling interface. First, we define the pressure by its mean value on each cell $[x_j, x_{j+1}[$:

$$p_{j+1/2}^{n+1} = \frac{1}{\Delta x}\{\Delta x_{j+1/2}^{*}p_{j+1/2}^{n+1-} - \Delta t(u_{j+1}^{n}p_{j+1+\alpha_{j+1,n}}^{n+1-} - u_j^n p_{j+\alpha_{j,n}}^{n+1-})\}, \quad j \in \{-1, 0\}.$$

Then, for $j \in \{-1, 0\}$, we define the total energy $(\rho E)^{n+1}_{j+1/2}$ by

$$(\rho E)^{n+1}_{j+1/2} = \frac{1}{2}\frac{\{(\rho u)^{n+1}_{j+1/2}\}^2}{\rho^{n+1}_{j+1/2}} + \rho^{n+1}_{j+1/2}\varepsilon(\rho^{n+1}_{j+1/2}, p^{n+1}_{j+1/2}) \,, \tag{17}$$

where $\varepsilon(\rho, p)$ refers to the left EOS for $j = -1$ and to the right EOS for $j = 0$.
With this new definition, the flux-coupling scheme preserves uniform pressure profiles. On the other hand, if it is still conservative for the density and the momentum, it cannot guarantee the conservation of energy as we stated in Section 3.1.

3.3 Intermediate State Coupling: Two Flux Scheme

We describe here the two flux scheme for the coupling problem (4). We generalize to this context the procedure proposed in Abgrall & Karni (2001). We choose two numerical flux functions $\mathbf{g_1}$ and $\mathbf{g_2}$ respectively consistent with the flux functions $\mathbf{f_1}$ and $\mathbf{f_2}$. We consider the following 3-points conservative schemes to solve numerically the systems on each side of the interface:

$$\begin{aligned} \mathbf{u}^{n+1}_{j-1/2} &= \mathbf{u}^n_{j-1/2} - \tfrac{\Delta t}{\Delta x}(\mathbf{g_1}_{,j} - \mathbf{g_1}_{,j-1}) \quad \underline{j \leq 0}, \\ \mathbf{u}^{n+1}_{j+1/2} &= \mathbf{u}^n_{j+1/2} - \tfrac{\Delta t}{\Delta x}(\mathbf{g_2}_{,j+1} - \mathbf{g_2}_{,j}), \quad \underline{j \geq 0}. \end{aligned} \tag{18}$$

with $\underline{\text{for all } j \neq 0}$:

$$\mathbf{g_1}_{,j} = \mathbf{g_1}(\mathbf{u}^n_{j-1/2}, \mathbf{u}^n_{j+1/2}), \quad \mathbf{g_2}_{,j} = \mathbf{g_2}(\mathbf{u}^n_{j-1/2}, \mathbf{u}^n_{j+1/2}). \tag{19}$$

The coupling of the the systems at the numerical level is done by the computation of the quantities $\mathbf{g_1}_{,0}$ and $\mathbf{g_2}_{,0}$. We need now to precise the information to be transmitted at the interface. We propose to identify the states at the interface by the state variables (ρ, u, p), which gives

$$\mathbf{g_1}_{,0} = \mathbf{g_1}(\mathbf{u}^n_{-1/2}, \overline{\mathbf{u}}^n_{1/2}), \quad \mathbf{g_2}_{,0} = \mathbf{g_2}(\overline{\mathbf{u}}^n_{-1/2}, \mathbf{u}^n_{1/2}). \tag{20}$$

with

$$\overline{\mathbf{u}}^n_{1/2} = (\rho^n_{1/2}, (\rho u)^n_{1/2}, (\overline{\rho E})^n_{1/2}), \quad \text{and} \quad (\overline{\rho E})^n_{1/2} = \tfrac{1}{2}\tfrac{(\rho u)^{n\,2}_{1/2}}{\rho^n_{1/2}} + \rho^n_{1/2}\varepsilon_1(\rho^n_{1/2}, p^n_{1/2}),$$

$$\overline{\mathbf{u}}^n_{-1/2} = (\rho^n_{-1/2}, (\rho u)^n_{-1/2}, (\overline{\rho E})^n_{-1/2}), \quad \text{and} \quad (\overline{\rho E})^n_{-1/2} = \tfrac{1}{2}\tfrac{(\rho u)^{n\,2}_{-1/2}}{\rho^n_{-1/2}} + \rho^n_{1/2}\varepsilon_2(\rho^n_{1/2}, p^n_{1/2}).$$

We remark that

$$(\overline{\rho E})^n_{1/2} \neq (\rho E)^n_{1/2} \quad \text{and} \quad (\overline{\rho E})^n_{-1/2} \neq (\rho E)^n_{-1/2}.$$

We also have, in general, that $\mathbf{g_1}(\mathbf{u}^n_{-1/2}, \overline{\mathbf{u}}^n_{1/2}) \neq \mathbf{g_2}(\overline{\mathbf{u}}^n_{-1/2}, \mathbf{u}^n_{1/2})$. Therefore, the scheme is not conservative in ρ, ρu and ρE.

4 NUMERICAL TESTS

We present here some numerical tests to better compare the three schemes we proposed in the previous sections.
The coupling problem we implemented is Problem (4) where, for the sake of simplicity, we considered as Equations of State, two perfect gas laws with different γ coefficients. We note γ_1 the constant which applies on the left domain and $p_1 = (\gamma_1 - 1)\rho\varepsilon$ the corresponding pressure. While γ_2 and $p_2 = (\gamma_2 - 1)\rho\varepsilon$ are the constant and pressure on the right domain.
For all the simulations we show here, we chose $\gamma_1 = 1.4$ and $\gamma_2 = 1.6$. This large gap between the

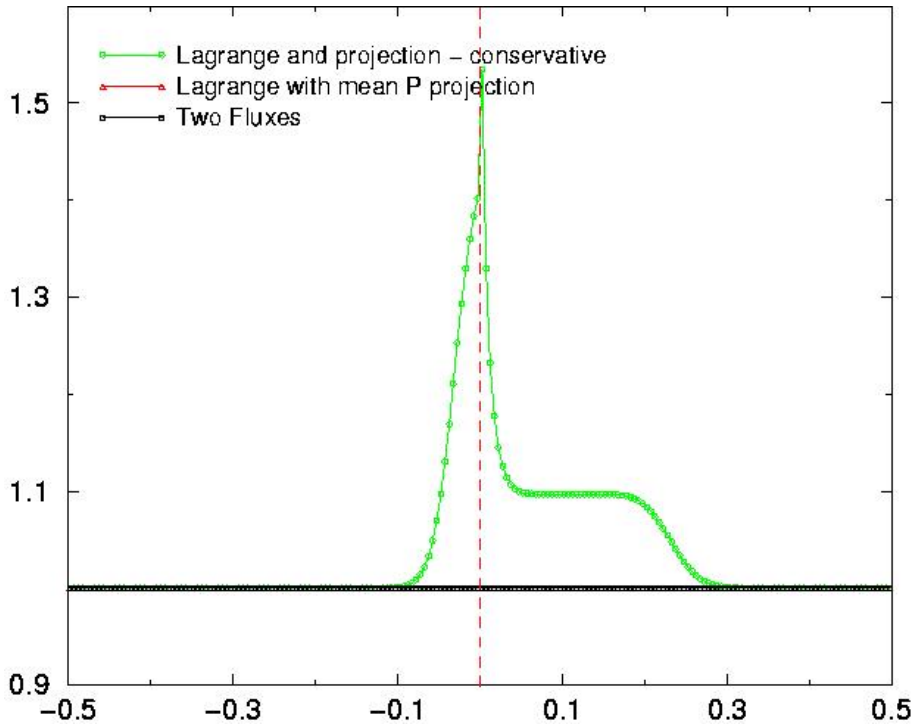

Figure 1: Steady state: Pressure profile at $t = 10^{-4}$

values of the two constants implies a big difference in the thermodynamic properties of the fluid on the left and on the right domain and was chosen to better spot the difficulties linked with the coupling procedure.

The first test we performed consists in taking the following uniform profile as initial condition:

$$\left\{ \begin{array}{rcl} \rho(x) & = & 1.0\,, \\ u(x) & = & 1.0\,, \\ p(x) & = & 1.0\,. \end{array} \right.$$

We expect this profile to be a steady state for the problem. The pressure and density profiles at $t = 10^{-4}$ are shown in Fig. 1 and Fig. 2. Clearly, the Lagrange+projection conservative scheme is unable to capture this solution and generates oscillations in the pressure profile therefore perturbing the whole solution.
On the other hand, if we look at the relative conservation error for the total energy (Fig. 3) versus time, the Lagrange+projection conservative scheme is the only one that conserves the total energy.
The Lagrange with mean pressure projection and the Two Fluxes schemes do not conserve the total energy, but the amplitude of this phenomenon is dependent on the discrepancy between the equations of state we considered. In Fig. 4, we show how the relative conservation error diminishes when considering smaller and smaller gaps in the equations of state (*i.e.* in the adiabatic coefficients γ).
This results well illustrate the discussion of Section 3.1.

In Section 3.1, we stated that a bad behavior in reproducing uniform pressure profiles is symptomatic of problems in computing material fronts propagation. We illustrate this assertion in Fig. 5 and Fig. 6 where we took the following initial condition

$$\left\{ \begin{array}{rcl} \rho(x) & = & \left\{ \begin{array}{ll} 1.0 & \text{for} \quad x < 0\,, \\ 2.0 & \text{for} \quad x > 0\,, \end{array} \right. \\ u(x) & = & 1.0\,, \\ p(x) & = & 1.0\,. \end{array} \right.$$

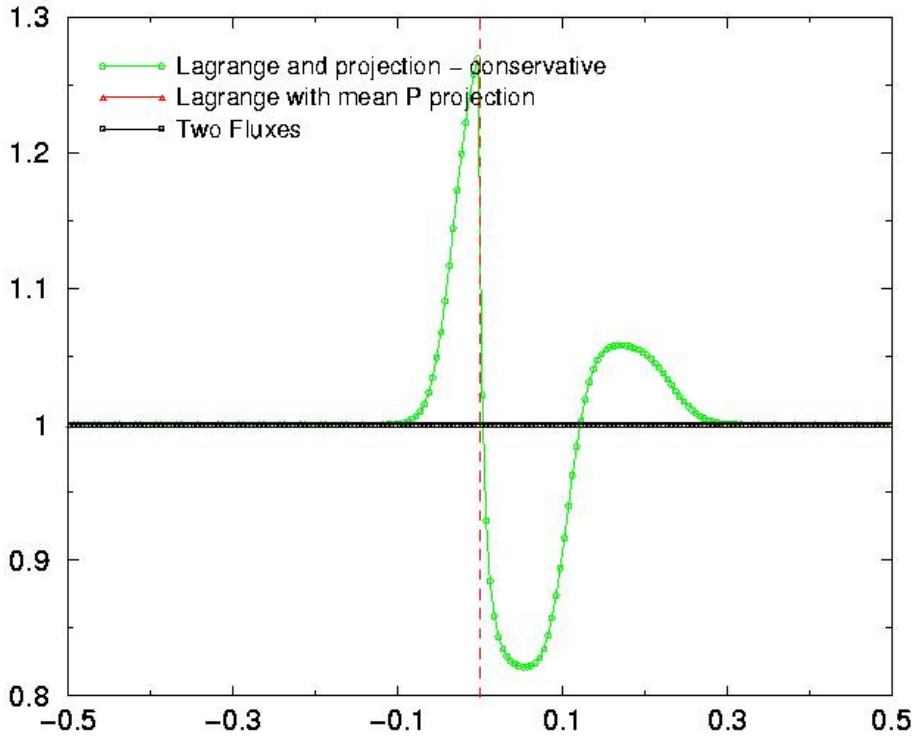

Figure 2: Steady state: density profile at $t = 10^{-4}$

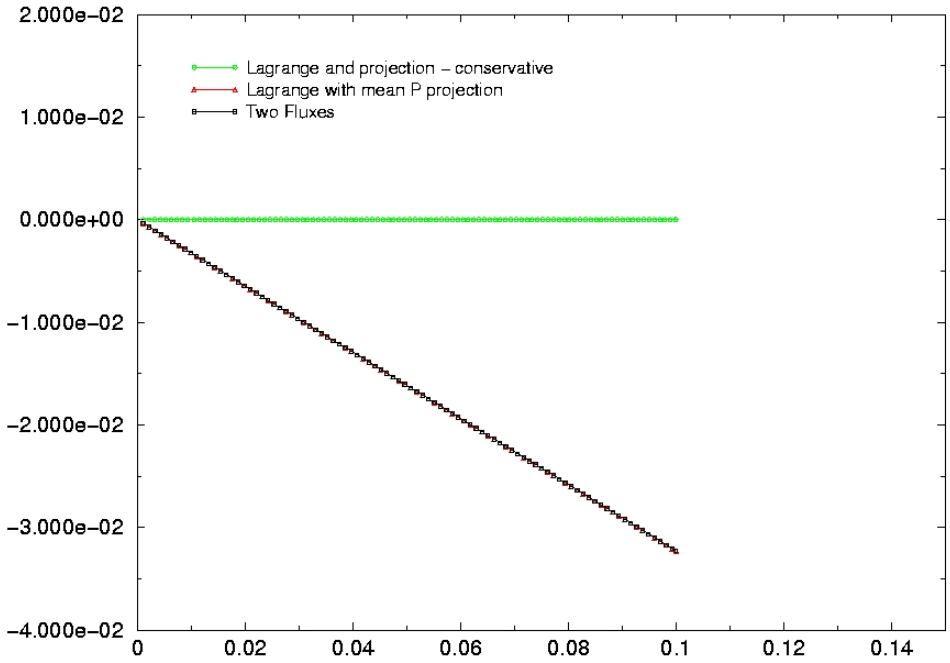

Figure 3: Steady state: relative conservation error for the energy versus time

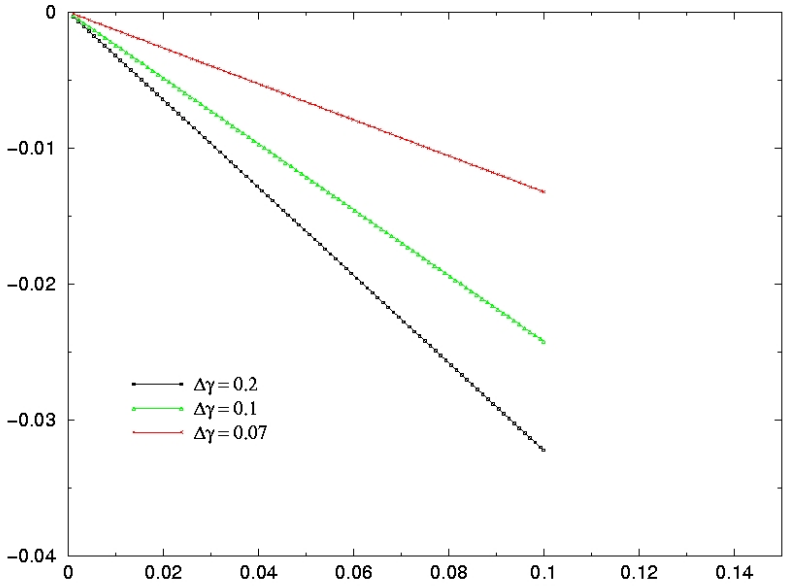

Figure 4: Steady state: relative conservation error for the energy versus time for the Lagrange with mean P projection and the Two Fluxes schemes for different jumps of the adiabatic constant

Again the Lagrange+projection conservative scheme cannot compute the solution correctly.

We also considered an example in which a rarefaction wave hits the interface corresponding to the discontinuity in the thermodynamic laws. As initial condition we consider a simple rarefaction wave which is entirely on the left domain and moves toward the right. If no discontinuity in γ were present, we would expect that the wave passes unaltered through the domain. The presence of the discontinuity in γ (*i.e.* the fact that this is a coupling problem) affects the transmission of the rarefaction wave and generates a reflected wave.
In Fig. 7, we plot the pressure profile at $t = 10^{-4}$, when the rarefaction wave has already entered the right domain. The density profile at $t = 10^{-4}$ is plotted in Fig. 8.
In Fig. 9, Fig. 10 and Fig. 11 we represent respectively the relative errors in the conservation of mass, momentum and energy. With no surprise, the Lagrange+projection conservative scheme is exactly conservative on all the three quantities, while the Two Fluxes scheme is conservative on neither of them. The Lagrange with mean pressure projection scheme is exactly conservative in ρ and ρu, but it can not conserve energy.

5 CONCLUSIONS

When computing a solution of a coupled problem, we are intervening on three stages. The first is on the level of the physical modelling, when we define which is the information to be transmitted at the interface. The second is linked with the analysis of the chosen coupled model, which can admit multiple solutions. Finally, problems can arise in the numerical approximation of the model.

In the problem we studied in this paper, we show how different modelling choices lead to different solutions. Clearly the problem is not on the numerical level, but it is really linked with the criteria that

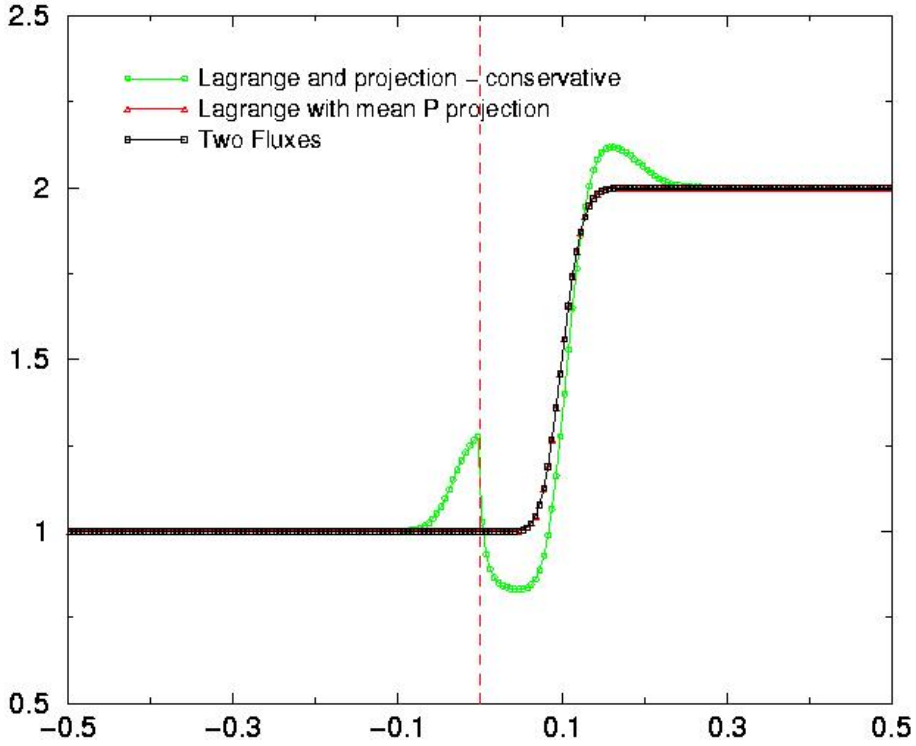

Figure 5: Material front: density profile at $t = 10^{-4}$

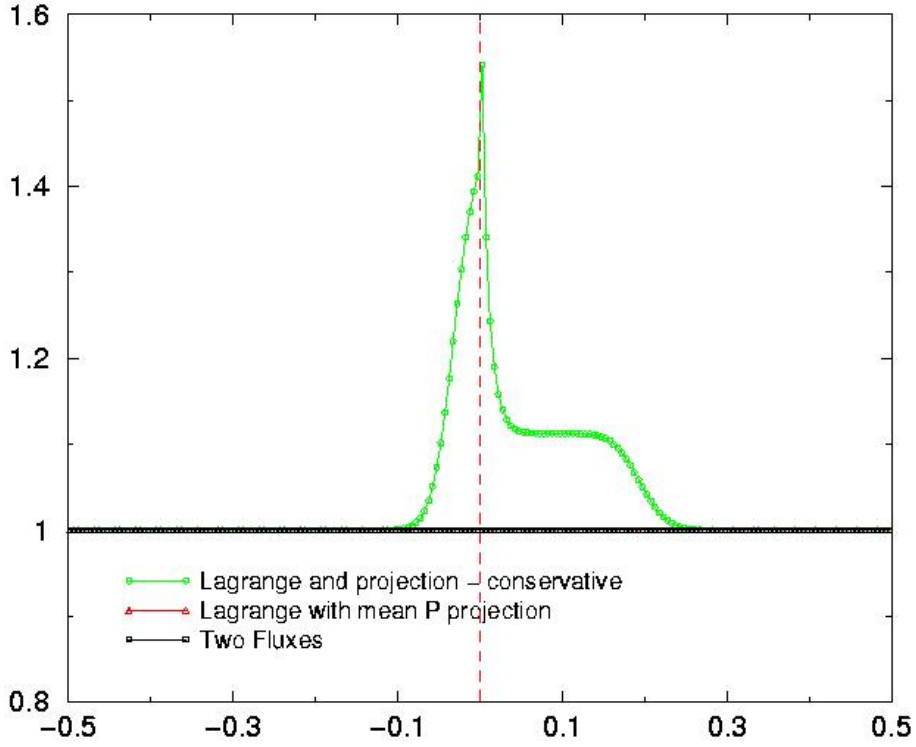

Figure 6: Material front: pressure profile at $t = 10^{-4}$

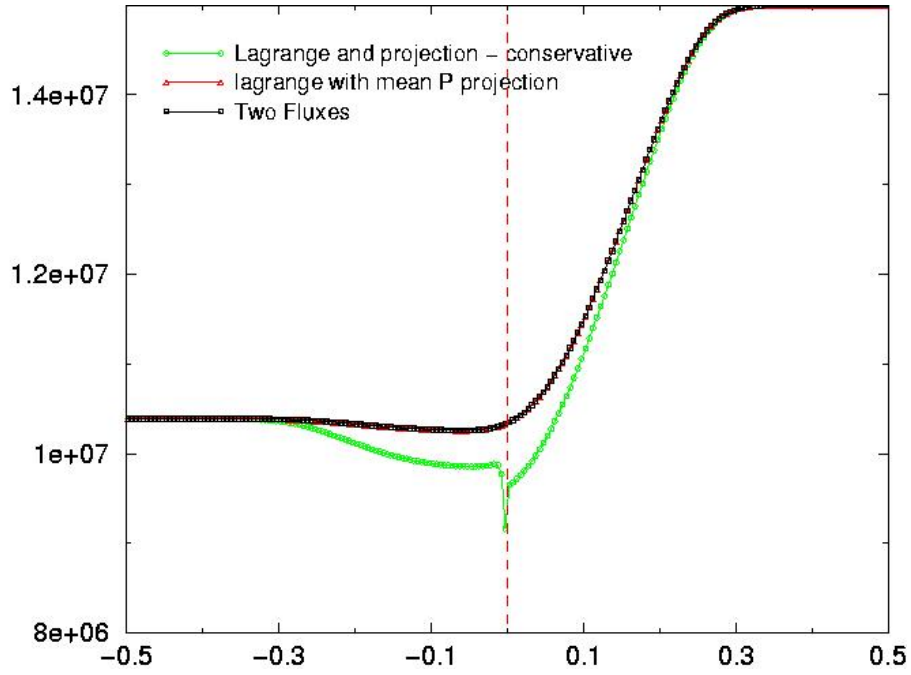

Figure 7: Rarefaction wave hitting the interface at $x = 0$: Pressure profile at $t = 10^{-4}$

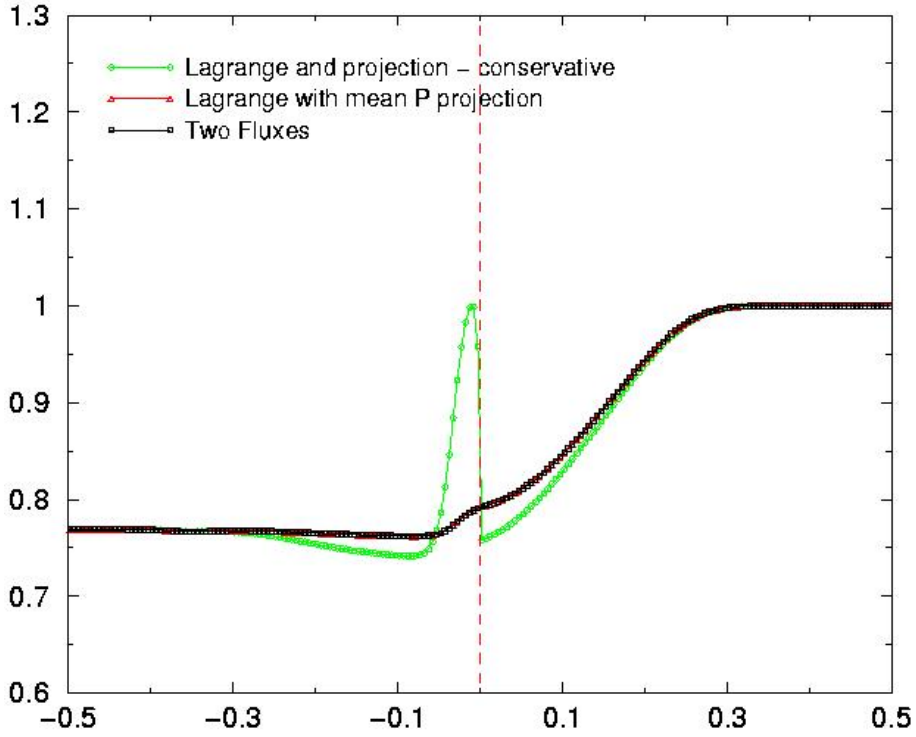

Figure 8: Rarefaction wave hitting the interface at $x = 0$: density profile at $t = 10^{-4}$

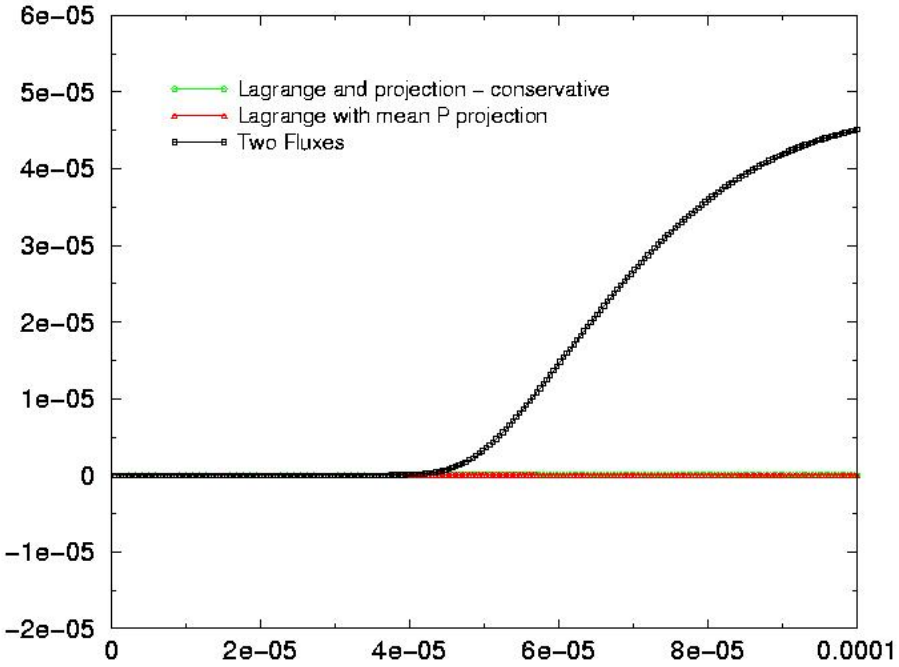

Figure 9: Rarefaction wave hitting the interface at $x = 0$: relative conservation error for the density versus time

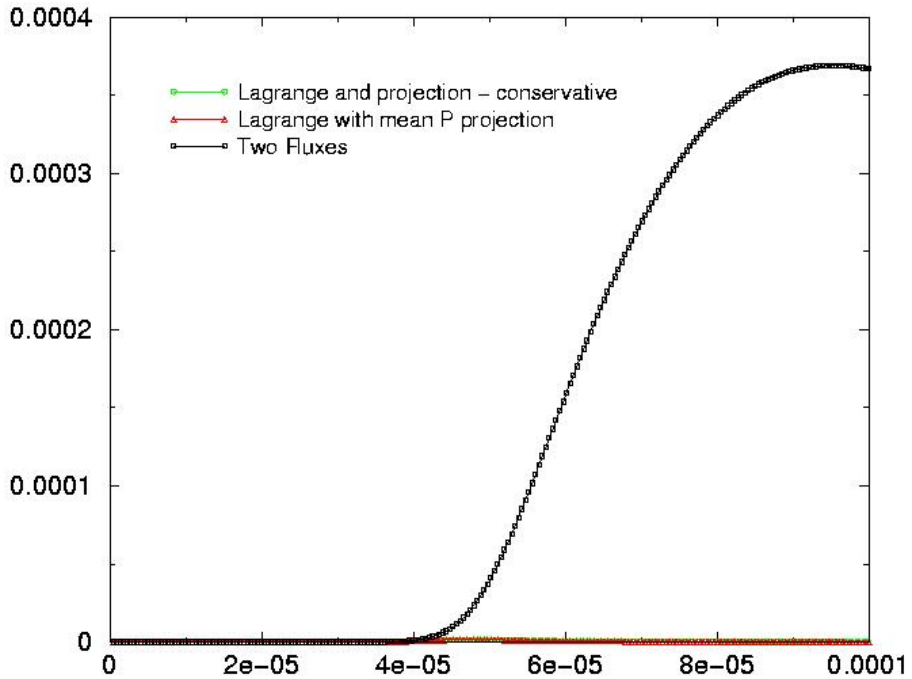

Figure 10: Rarefaction wave hitting the interface at $x = 0$: relative conservation error for the flow rate versus time

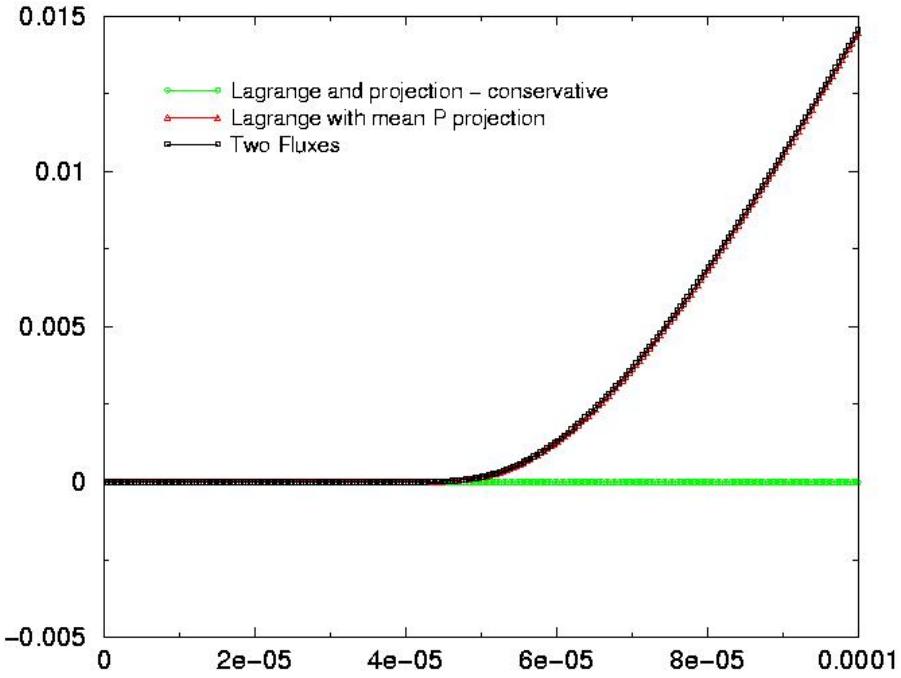

Figure 11: Rarefaction wave hitting the interface at $x = 0$: relative conservation error for the energy versus time

one wants to impose to the global model, *i.e*. preservation of uniform pressure profiles *versus* strict conservation of energy, in this example.

The general coupling of two-phase flow models is under study. One of our goals is the coupling between a THYC model with a CATHARE one.

REFERENCES

Abgrall, R., & Karni, S. 2001. Computations of compressible multifluids. *Journal of Computational Physics*, 169:594–623.

Ambroso, A., Chalons, C., Coquel, F., Godlewski, E., Lagoutière, F., Raviart, P.-A., & Seguin, N. 2005. *Joint CEA-SFME / Laboratoire Jacques-Louis Lions Working Group on the Coupling of Models in Thermal Hydraulics.*

Boudier, P., & Laviéville, J. 2004. Pressurized Thermal Shock Calculations:Test of Coupling System and Local 3D Scales. *CATHARE-NEPTUNE International Seminar, May 10-12, Grenoble, France (unpublished).*

Godlewski, E., & Raviart, P.-A. 1996. *Numerical Approximation of Hyperbolic Systems of Conservation Laws*. New York: Springer-Verlag.

Godlewski, E., & Raviart, P.-A. 2004. The numerical interface coupling of nonlinear hyperbolic systems of conservation laws: I the scalar case. *Numerische Mathematik*, **97**, 81–130.

Godlewski, E., Le Thanh, K.-C., & Raviart, P.-A. 2005. The numerical interface coupling of nonlinear hyperbolic systems of conservation laws: II the case of systems. *to appear in Math. Mod. and Num. Anal.*

Greenberg, J.M., & LeRoux, A.Y. 1996. A well-balanced scheme for the numerical processing of source terms in hyperbolic equations. *SIAM J. Numer. Anal.*, **33**, 1–16.

Guelfi, A. et al. 2005. A New multi scale platform for advanced nuclear thermal hydraulics. Status and prospects of the NEPTUNE project. *to appear in the proceedings of NURETH11.*

Hérard, J.M. 2004. Naive schemes to couple isentropic flows between free and porous medium. *EDF internal report HI-81/04/08/A.*

Hérard, J.M., & Hurisse, O. 2004a. Coupling one and two-dimensional models through a thin interface. *EDF internal report HI-81/05/01/A.*

Hérard, J.M., & Hurisse, O. 2004b. A few schemes to compute unsteady hyperbolic systems with source terms. *EDF internal report HI-81/04/07/A.*

Hurisse, O. PhD Thesis. *In preparation.*